Organic & Biomolecular Chemistry RSCPublishing

EDGE ARTICLE

# The Importance of Chain Conformational Mobility During *5-Exo*-Cyclizations of *C*-, *N*- and *O*-Centred Radicals†

Cite this: DOI: 10.1039/x0xx00000x

Received 00th January 2012,
Accepted 00th January 2012

DOI: 10.1039/x0xx00000x

www.rsc.org/

John C. Walton[a]

The reaction coordinates of an archetypical set of *5-exo* cyclizations of *C*-, *N*- and *O*-centred radicals were investigated by computational methods. G4 theory, and DFT with the um062x functional, were able to rationalise counterintuitive factors such as the 'normal' order of rate constants being: *N*-centred < *C*-centred < *O*-centred radicals. The access angle between the radical centre and the double bond was identified as a key factor. Examination of its evolution during ring closure implied that rigidity at the *N*-ends of the chains, and the consequent extra energy needed to attain chair-like transition states, might be the reason for slow aminyl cyclizations. A novel linear correlation between cyclization activation energies and the access angles was discovered. The preference for *cis*-1,2-disubstituted product formation was also accounted for in terms of interaction between the hyperconjugatively delocalized SOMO and the alkene π* orbital.

## Introduction

It is well established that neutral radicals having alkene acceptor groups at the 5-position with respect to the radical centre (**1**) regioselectively ring close in the *5-exo-trig* mode to afford 5-member ring containing products (**3**). This property has been exploited in many organic synthetic procedures,[1] in natural product syntheses,[2] and in numerous tandem and cascade processes.[3] The main characteristics of the reaction were delineated in a seminal article by Beckwith and Ingold in 1980.[4]

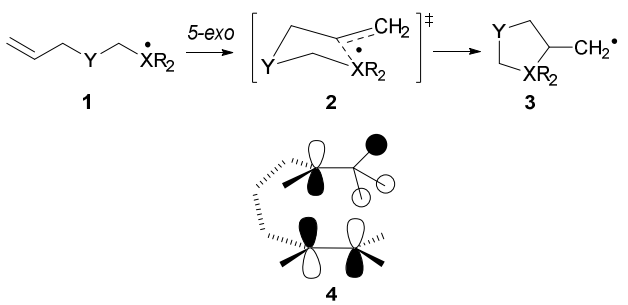


**Scheme 1**

The quality of kinetic data for radical ring closures remains rather variable, but a considerable body of such information is now available for *C*-centred hex-5-enyl type radicals[4,5,6] and more is steadily becoming available for carbonyl radicals,[7,8] *N*-centred aminyl[9,10,11] and iminyl radicals,[12,13] for a few *O*-centred species such as pent-4-enyloxyl[14,15] and for allyloxycarbonyloxyl radicals.[16] The entropy of activation favors 5-member ring rather than 6-member ring formation, but this factor is too small to account for the much higher *5-exo* closure rates in comparison with *6-endo*; instead control resides with the activation enthalpy terms. For the *C*-centred hex-5-enyl series, alkyl substituents at either the 1- or 6-positions had only a minor effect on the rate. In sharp contrast, substituents at the 5-position dramatically reduced the *5-exo*-rate and often diverted ring closure into the *6-endo-trig* mode. Di-substitution at the 2- or 3-positions substantially increased the rate of the *5-exo* ring closure, thus providing examples of radical *gem*-dialkyl effects. Similarly, replacement of $CH_2$ with an *O*-atom at the 3-position also induced a significant increase in cyclization rate. Counterintuitively, hex-5-enyl types with a single methyl substituent at the radical centre yielded mixtures of *cis*- and *trans*-disubstituted 5-member ring compounds containing a preponderance of the *cis*-isomers. The reason for this was suggested to be a secondary attractive interaction in the transition state (TS), between the radical SOMO (hyperconjugatively delocalized to the incipiently *cis*-Me substituent) and the alkene π* orbital (see structure **4**).[17]

Kinetic and stereo-chemical results from radical ring closures have usually been rationalized by reference to the Beckwith-Houk transition state.[18,19] For *5-exo*-closures this TS resembles the comparatively strain-free chair conformation of

the cyclohexane ring **2** with the radical centre (X-1) approaching C-5 of the alkene at an angle close to tetrahedral. A number of computational studies of hex-5-enyl ring closures have been reported[20-24] and these have generally supported Beckwith-Houk type TS models. Computational studies of the ring closures of carbonyl radicals,[25] iminyl radicals,[13] aminyl radicals[26] and oxyl radicals[15] have generally focused either on the *exo* vs. *endo* regioselectivity or on details of the stereochemistry induced by substituents.

A recent appraisal of rate constants for *5-exo* cyclizations of model *N*-, *C*-, and *O*-centred alkenyl type radicals ($k_c$/s$^{-1}$ at 300 K in hydrocarbon solutions) showed that they span at least 5 orders of magnitude.[27] Intriguingly the magnitude of $k_c$ depended strongly on the nature of the radical-bearing atom. For an archetype set, the *N*-centred species, including aminyl and iminyl, cyclized the slowest ($k_c < 10^4$ s$^{-1}$) *C*-centred, including alkyl and acyl, cyclized at intermediate rates ($10^6 > k_c > 10^5$ s$^{-1}$) and *O*-centred were fastest ($k_c > 10^7$ s$^{-1}$). Values outside these ranges are, of course, possible for radicals with more exotic substituents but the 'normal' order is:

*N*-centred < *C*-centred < *O*-centred

Unexpectedly, these rate constants did not line up according to the sequence of the radical centres in the first row of the Periodic Table (electronegativity order). The results of an investigation to see if current ab initio and DFT theoretical methods could reproduce these counterintuitive trends, and what insights could be obtained into their causes, are reported in this paper.

## Results and Discussion

### Experimental Kinetic Data for *5-exo* Cyclizations

Experimental kinetic data is collected in Table 1 for *5-exo*-cyclizations of a set of archetype radicals. This set was chosen because the data, though far from perfect, is amongst the most reliable and because it illustrates the effects of key structural features. Large differences in the entropies of activation are not expected for this set of similar reactions and, where available, the measured log[$A_c$/s$^{-1}$] were all 10±0.5 (see Table 1 and refs. 4-6). In a few cases (Table 1) activation energies were therefore estimated from reported rate constants, assuming log($A_c$) of this magnitude. Two types of *N*-centred radicals, aminyl (**5e**) and iminyl (**6e**), are included together with two types of *O*-centred radicals, alkoxycarbonyloxyl (**13e**) and alkoxyl (**14e**). The *C*-centred types include the archetype hex-5-enyl (**7e**), plus radical **10e** with two methyl substituents at the radical centre, **11e** with a 3-oxa-substituent and acyl type **12e.** The *5-exo*- ring closures of **8e** (**8e** and **9e** are, of course, the same open chain radical when extended) were specially chosen to probe the ability of computational methods to rationalize the unexpected faster rate of *cis*-1,2-disubstituted-5-member ring formation as compared to *trans* (Table 1).

**Table 1.** Experimental rate constants and Arrhenius activation parameters for *5-exo* cyclizations of hex-5-enyl type radicals.

| Cyclization | $k_c$/s$^{-1}$ 298 K[a] | Log($A_c$/s$^{-1}$) | $E^{\ddagger}$ / kJ/mol | Ref. |
|---|---|---|---|---|
| 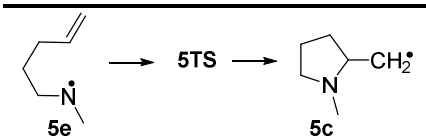 5e 5TS 5c | $3.0 \times 10^3$ | [10.5] | [39.4][b] | 11,6 |
| 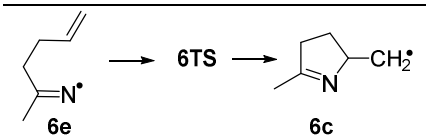 6e 6TS 6c | $1.0 \times 10^4$ | [10.5] | [38.5][b] | 6,13 |
| 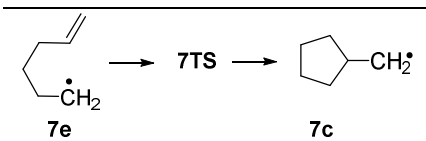 7e 7TS 7c | $2.3 \times 10^5$ | 10.4 | 28.6 | 28 |
| 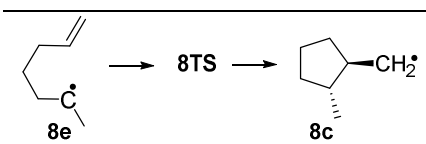 8e 8TS 8c | $2.9 \times 10^4$ | 9.92 | 31.1 | 29 |
| 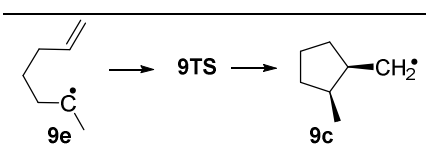 9e 9TS 9c | $1.0 \times 10^5$ | 9.79 | 27.2 | 29 |

| | | | | |
|---|---|---|---|---|
| 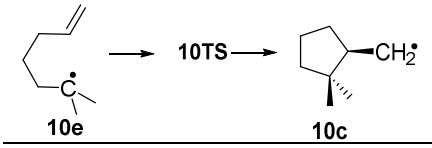 10e 10TS 10c | $3.3 \times 10^5$ | 10.0 | 25.5 | 29 |
| 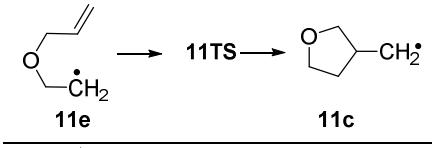 11e 11TS 11c | $9.0 \times 10^6$ | 9.9 | 16.7 | 30 |
| 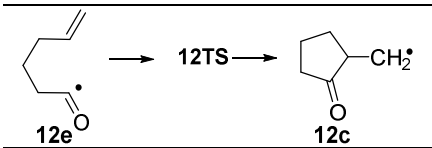 12e 12TS 12c | $2.2 \times 10^5$ | 9.6 | 25.1 | 31 |
| 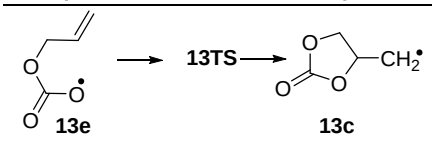 13e 13TS 13c | $1.0 \times 10^7$ | [10.5] | [21.7][c] | 16 |
|  14e 14TS 14c | $4.0 \times 10^8$ | [10.5] | [11.5][c] | 14 |

[a] The $k_c$ all refer to $T$ at, or close to, 298 K. [b] Projected from data from the corresponding 2-Ph and 2-Bu species. [c] Estimated on the assumption that $\log[A_c/s^{-1}] = 10.5$

.

**Choice of Computational Methods**

All calculations used the Gaussian09 suite of programs.[32] Initial geometry optimizations were performed using the UB3LYP hybrid density functional with the 6-31+G(d) basis set. Further full geometry optimizations were carried out at every level of theory used. Minima and transition states were confirmed as such by calculating their normal vibrations at each level of theory. All transition states had one imaginary frequency that corresponded to the reaction coordinate. The zero-point energies and thermal corrections to 298 K derived from these calculations were used for the computation of thermodynamic quantities in the standard state [$\Delta H°$, $\Delta G°$ etc.]. After annihilation $<s^2>$ values were all 0.750±0.001 and hence quartet contamination was negligible.

For the trial set of cyclizations shown in Table 2, geometries, reaction enthalpies and activation enthalpies were computed with the UB3LYP functional and the 6-311+G(2d,p) basis set, also with Dunning's correlation consistent triple-zeta basis set with added diffuse functions, aug-cc-pvtz[33,34] and with the CBS-QB3/6-311G(2d,p) complete basis set method.[35] Although the B3LYP functional generally gives reasonable agreement with experiment for reactions of radicals based on first-row elements, it usually underestimates activation barriers[36] and makes no provision for dispersion forces. Results were therefore also computed with the fourth generation G4 method[37] and with the hybrid m062x functional of Truhlar that includes dispersion corrections.[38] The trial set (Table 2) was chosen to give a reasonable cross-section of the radical cyclization processes and so includes an *N*-centred radical (**5e**), a *C*-centred radical (**7e**) and an *O*-centred radical (**14e**) as well as the recently investigated species **13e**. The extended all-*trans* conformations were found to be energy minima for all the radicals and reaction enthalpies and activation energies were calculated relative to these ground states. However, in solution and vacuum, the radicals populate a set of conformations involving partial internal rotations about the backbone C-C bonds. Experimental thermodynamic parameters will relate to an appropriate average and hence the computed values may somewhat overestimate them.

**Table 2.** Cyclization Enthalpies ($\Delta H°$/kJ mol$^{-1}$) from a Selection of Computational Methods

| Ring Closure | UB3LYP/6-311+G(2d,p) | UB3LYP/ aug-cc-pvtz | CBS-QB3 | um062x/6-311+G(2d,p) | G4 | Zavitsas GA[a] |
|---|---|---|---|---|---|---|
| **5e → 5c** | -9.1 | -8.7 | -41.9 | -41.4 | -38.9 | [-49.7] |
| **7e → 7c** | -40.4 | -44.3 | -65.6 | -61.4 | -62.2 | -64.0 |
| **13e → 13c** | -50.2 | -46.9 | -73.2 | -86.5 | -72.9 | – |
| **14e → 14c** | -39.1 | -39.8 | -67.0 | -63.1 | -63.1 | -66.9 |

[a] Empirical Group Additivity values – see text.

All 5 methods predict the *5-exo*-cyclizations of *N*-, *C*- and *O*-centred radicals will be exothermic. The UB3LYP functional, with both the 6-311+G(2d,p) and aug-cc-pvtz basis sets, predicts significantly smaller magnitude $\Delta H°$ values than the more advanced methods. The CBS-QB3, um062x and G4 methods show a consistent picture with the smallest $\Delta H°$ for *N*-centred radical **5e**, an intermediate value for *C*-centred radical

**7e** and the highest exothermicities for the *O*-centred radicals **13e** and **14e**. This places the cyclizations in the correct order of reactivity.

The experimental enthalpies of formation ($\Delta_f H°$) are not available for both reactant and cyclized radicals of the sets in Table 2. However, Group Additivity (GA) schemes deliver this data for hydrocarbon *C*-centred radicals and a few others. Such schemes have recently been reviewed by Zavitsas[39] who recommended a simple relationship for hydrocarbon radicals based on the known $\Delta_f H°$ values of the corresponding hydrocarbons.[40] The $\Delta H°$ obtained from Zavitsas relationship for ring closure of radical **7e** is in Table 2 and will be close to the 'true' value (± 3 kJ/mol, see ref. 39) because this relationship is derived from a lot of experimental data. The GA value of $\Delta H°$ for the *O*-centred system **14e** should also be reasonably reliable. However, for the *N*-centred system **5e**, very little experimental $\Delta_f H°$ data on aminyl radicals is available, and it all relates to primary aminyl radicals, whereas **5e** is a secondary aminyl radical. It follows that the GA $\Delta H°$ in Table 2 for **5e** is little better than guesswork. It is clear from Table 2 that the $\Delta H°$ values computed by all three CBS-QB3, um062x and G4 methods are in good agreement with the GA values whereas the UB3LYP methods underestimate $\Delta H°$.

**Computation of Activation Parameters and Transition States**

In view of its good success in the benchmarking described above, the full G4 method was applied to the computation of transition states and activation parameters for all the cyclizations of Table 1. The um062x functional consumed much less computing resources so it was also applied so as to further assess its suitability. The enthalpies of activation ($\Delta H^{‡}$) and reaction enthalpies ($\Delta H°$) obtained from the two methods are displayed in Table 3. There is reasonable agreement between the two computational methods, for both thermodynamic parameters, with the exception of the two *O*-centred cyclizations **13e** and **14e**. The data is shown plotted against the experimental Arrhenius activation energies $E^{‡}$ in Figure 1. On comparing with the line of unit slope it is seen that for both methods the computed $\Delta H^{‡}$ values are generally greater than the experimental Arrhenius $E^{‡}$ by averages of 6.5 kJ/mol (G4) and 9.4 kJ/mol (um062x).

The experimental rate parameters were all obtained for solution phase experiments carried out in non-polar benzene or *t*-butylbenzene solvents. Solvent effects were, therefore, expected to be small. To check on this factor, both $\Delta H°$ and $\Delta H^{‡}$ were re-examined for a selection of N-, C- and O-centred radicals using the G4 method with full geometry optimization and the CPCM polarizable conductor calculation model including benzene as solvent (see Table 3, columns 4 and 5). With the exception of the more polar **13e** system, the presence of solvent made < ~ 3 kJ/mol difference to either computed $\Delta H°$ or $\Delta H^{‡}$. There was no systematic trend and the larger magnitude of the computed $\Delta H^{‡}$, in comparison with the experimental $E^{‡}$, could not be attributed to solvent effects

**Figure 1**(a): Plot of computed $\Delta H^{‡}$ vs. experimental Arrhenius activation energies ($E^{‡}$).
**1**(b): Plot of $\Delta H°$ vs. experimental & computed activation enthalpies ($E^{‡}$, $\Delta H^{‡}$).

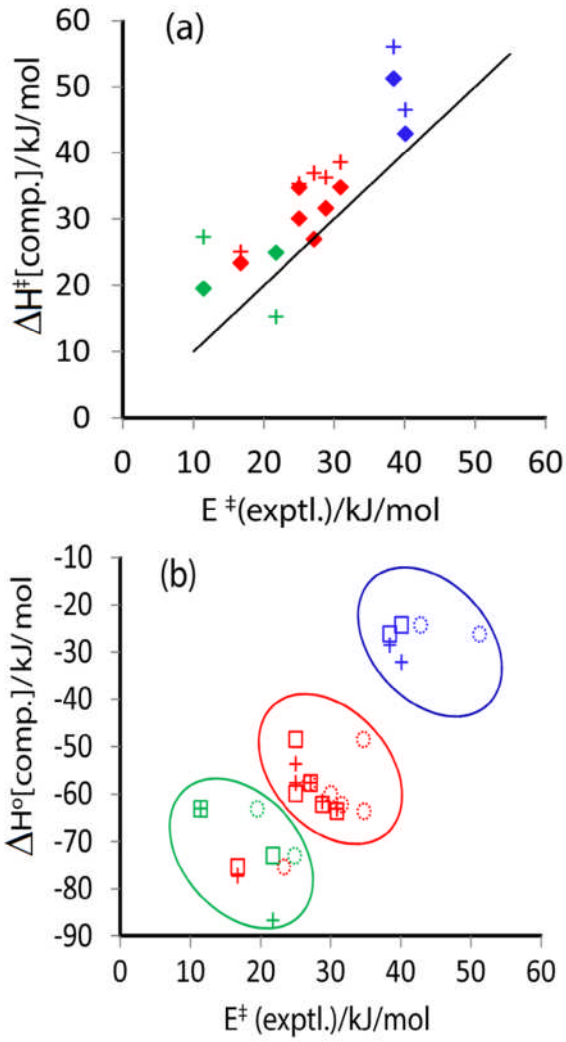


In Figure **1(a)**: Diamonds: G4 computed values; Crosses: um062x computed values. The full line is that of unit slope.
In Figure **1(b)**: Squares: G4 computed values vs exptl. $E^{‡}$; Crosses um062x computed values vs exptl. $E^{‡}$; Circles: G4 computed $\Delta H°$ vs G4 computed $\Delta H^{‡}$. In each case blue signifies *N*-centred, red signifies *C*-centred and green signifies *O*-centred radicals.

As mentioned above, a possible factor contributing to the higher $\Delta H^{‡}$ is that they were computed relative to the extended conformations of the open chain radicals. Clark and co-workers[22] found that for ring closure of the hex-5-enyl radical **7e** the activation enthalpy was lower by ~5 kJ/mol when computed relative to a local minimum "precursor" conformation resembling that of the TS. As a check on this factor, local minimum "precursor" structures were sought and found for most of the radicals using the um062x method. The activation enthalpies relative to these precursor conformations ($\Delta H^{‡}_{PR}$) are also displayed in Table 3. The um062x method for hex-5-enyl found only a lowering 0.4 kJ/mol in activation

enthalpy. For all the other radicals (except **11e**) the difference in $\Delta H^{\ddagger}_{PR}$ and $\Delta H^{\ddagger}$ was < 5 kJ/mol. In several cases (**8e**, **12e, 13e** and **14e**) $\Delta H^{\ddagger}_{PR}$ was marginally higher than $\Delta H^{\ddagger}$ because the precursor conformations were slightly lower in energy than the extended conformations. It follows that the higher computed $\Delta H^{\ddagger}$ values can't be simply explained by relating the TSs to the precursor conformations.

**Table 3.** Reaction Enthalpies ($\Delta H°$) and Activation Enthalpies ($\Delta H^{\ddagger}$) for Radical *5-Exo* Ring Closures Computed with Two Methods

| Ring Closure | $\Delta H°$ G4 | $\Delta H^{\ddagger}$ G4 | $\Delta H°$ G4(PhH)[a] | $\Delta H^{\ddagger}$ G4(PhH)[a] | $\Delta H°$ um062x | $\Delta H^{\ddagger}$ um062x | $\Delta H_{PR}^{\ddagger}$ um062x |
|---|---|---|---|---|---|---|---|
| **5ec → 5cc**[b] | -24.29 | 42.85 | – | – | -32.9 | 46.52 | 43.3 |
| **5et → 5ct**[c] | -38.87 | 56.93 | -35.36 | 58.14 | -41.38 | 62.32 | |
| **6e → 6c** | -26.21 | 51.25 | -24.45 | 50.91 | -28.55 | 56.05 | 53.8 |
| **7e → 7c** | -62.24 | 31.60 | -61.11 | 32.06 | -61.57 | 36.24 | 35.8 |
| **8e → 8c** | -63.66 | 34.78 | – | – | -63.16 | 38.54 | 39.8 |
| **8e → 9c** | -57.68 | 26.96 | – | – | -57.64 | 36.91 | |
| **10e → 10c** | -59.94 | 30.05 | -58.90 | 30.43 | -57.73 | 35.32 | 31.5 |
| **11e → 11c** | -75.37 | 23.37 | -75.11 | 23.87 | -77.33 | 25.04 | 9.5 |
| **12e → 12c** | -48.53 | 34.69 | -50.91 | 34.15 | -53.67 | 29.97 | 32.9 |
| **13e → 13c** | -72.94 | 24.91 | -81.51 | 17.51 | -86.69 | 15.26 | 16.1 |
| **14e → 14c** | -63.12 | 19.52 | -62.03 | 19.48 | -63.08 | 27.30 | 30.7 |

[a] G4 computation with the CPCM polarizable conductor calculation model and benzene as solvent. [b] Cyclization of *N*-methylpent-4-en-1-aminyl **5e** via a chair TS with the *N*-Me and $CH_2$ *cis.* [c] Cyclization of *N*-methylpent-4-en-1-aminyl to yield *N*-methylpyrrolidinylmethyl radical **5c** as the *trans*-isomer.

Figure 1 shows that both computational methods sorted the ring closure rates in the correct, counterintuitive, order with *N*-centred slower than *C*-centred slower than *O*-centred (see Figure 1) with only one exception (**11e**). In view of this these computed results seemed a satisfactory basis for deeper analysis. Linear regression gave the following relationships:

$$\Delta H^{\ddagger}(\text{G4}) = 1.15E^{\ddagger} + 2.38 \quad (R^2 = 0.831) \qquad (1)$$

$$\Delta H^{\ddagger}(\text{um062x}) = 1.24E^{\ddagger} + 2.63 \quad (R^2 = 0.725) \qquad (2)$$

The correlation of $\Delta H^{\ddagger}_{PR}$ with $E^{\ddagger}$ was significantly poorer. It appeared from Figure 1a that the G4 method handled the *N*-centred and the *O*-centred radicals somewhat more adequately than the um062x functional.

Reaction enthalpies play an important role in controlling many types of radical processes. To check on this factor, the experimental data was plotted against the computed $\Delta H°$ values with the result shown in Figure 1(b). This reveals a rough trend in which the more exothermic cyclizations tend to have lower activation energies. Again both computational methods correctly sort the processes into zones for each type of radical (circled in blue, red and green for *N*-, *C*- and *O*-centred) with the exception of **11e**. In case the scatter was due to errors in the experimental rate data, a plot of the computed $\Delta H^{\ddagger}$ vs the computed $\Delta H°$ values is included in Figure 1(b) (circles). It is clear from this that the scatter cannot be attributed to large experimental error limits because theory also predicts no simple Evans-Polanyi type relationship for *5-exo* cyclizations. Correlations of experimental with computed activation parameters have been noted previously[41,42] for radical and nucleophilic ring closures. In these studies derivations of intrinsic activation energies via Marcus Theory suggested that deviations from such correlations usually indicate the presence of specific TS-stabilizing effects.

### Transition State and Reaction Coordinate Properties

The structures and frontier orbitals (alpha SOMOs) of the TSs of selected radicals, computed with the G4 method, are shown in Figure 2 (see ESI for a complete set of structures). The structures for *N*-centred aminyl (**5TS),** *C*-centred **7TS - 11TS** and acyl **12TS,** as well as *O*-centred alkoxyl **14TS** all resemble the cyclohexane chair-like form of the Beckwith-Houk model (**2**). The exceptions are, of course, for the iminyl (**TS6**) and alkoxycarbonyloxyl (**13TS**) which show flattening of the ring in the region of their double bonds. The radical centres are strategically placed above the alkene double bonds with approach angles not greatly different from tetrahedral. The TS SOMOs show moderate interaction of the π- or σ-orbital of the radical centre with the alkene π-system. The latter retain much of their π-character in the TSs. Some key structural parameters for each TS and each 5-member ring product radical are listed in Table 4.

**Figure 2**. Structures and SOMOs of Selected Transition States Computed at the G4 level.

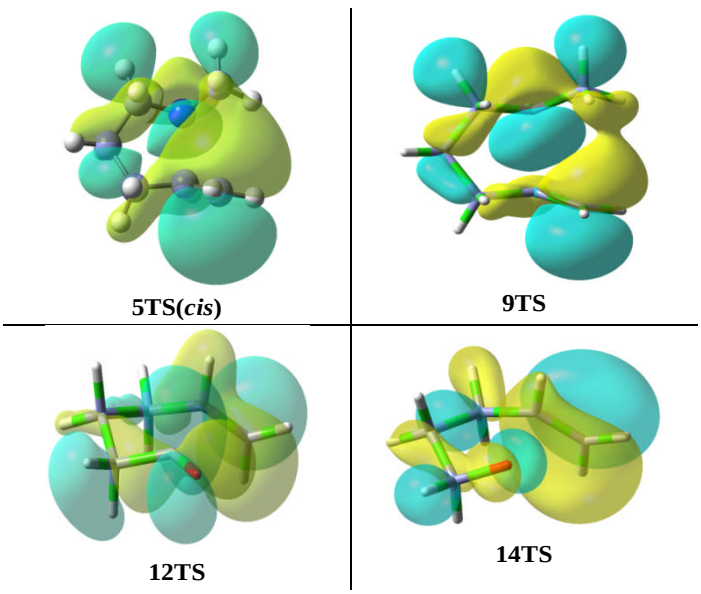

**Table 4.** G4 computed structural parameters for *5-exo* TSs, precursor conformations (PR) and 5-member ring product radicals. [a]

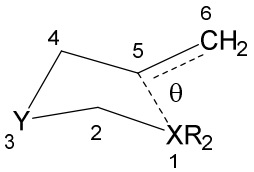


| Species | $d_{1,5}$ | $\delta d_{1,5}$ | $d_{5,6}$ | $\delta d_{5,6}$ | $d_{1,2}$ | $\delta d_{1,2}$ | θ | $\delta\theta_T$ |
|---|---|---|---|---|---|---|---|---|
| **5TS(*cis*)** | 2.014 | | 1.382 | | 1.446 | | 109.4 | |
| **5PR(cis)** | 2.925 | | 1.326 | | 1.442 | | 106.0 | |
| **5TS(*trans*)** | 2.050 | | 1.376 | | 1.447 | | 110.7 | |
| **5PR(trans)** | 3.090 | | 1.325 | | 1.440 | | 140.8 | |
| **5c(*trans*)** | 1.468 | 0.546 | 1.485 | 0.103 | 1.458 | 0.012 | 112.4 | 3.0 |
| **6TS** | 2.042 | | 1.378 | | | | 109.6 | |
| **6PR** | 3.273 | | 1.324 | | | | 82.4 | |
| **6c** | 1.477 | 0.565 | 1.487 | 0.109 | | | 111.8 | 2.2 |
| **7TS** | 2.262 | | 1.367 | | 1.499 | | 109.5 | |
| **7PR** | 3.063 | | 1.326 | | 1.488 | | 105.3 | |
| **7c** | 1.549 | 0.714 | 1.484 | 0.117 | 1.547 | 0.048 | 115.0 | 5.5 |
| **8TS** | 2.240 | | 1.369 | | 1.501 | | 110.0 | |
| **8PR** | 3.034 | | 1.326 | | 1.491 | | 104.6 | |
| **8c** | 1.560 | 0.680 | 1.484 | 0.115 | 1.539 | 0.038 | 115.2 | 5.2 |
| **9TS** | 2.234 | | 1.371 | | 1.502 | | 110.4 | |
| **9c** | 1.570 | 0.680 | 1.484 | 0.113 | 1.540 | 0.038 | 116.6 | 6.2 |
| **10TS** | 2.211 | | 1.375 | | 1.512 | | 110.8 | |
| **10c** | 1.579 | 0.632 | 1.483 | 0.108 | 1.545 | 0.033 | 116.6 | 5.7 |
| **11TS** | 2.284 | | 1.361 | | 1.495 | | 111.2 | |
| **11PR** | 3.002 | | 1.325 | | 1.486 | | 109.8 | |
| **11c** | 1.551 | 0.733 | 1.482 | 0.121 | 1.539 | 0.044 | 115.3 | 4.1 |
| **12TS** | 2.219 | | 1.367 | | 1.518 | | 107.7 | |
| **12PR** | 2.989 | | 1.325 | | 1.522 | | 96.3 | |
| **12c** | 1.567 | 0.652 | 1.480 | 0.113 | 1.531 | 0.013 | 114.0 | 6.4 |
| **13TS** | 2.121 | | 1.358 | | 1.355 | | 104.2 | |
| **13PR** | 3.264 | | 1.323 | | | | 85.8 | |
| **13c** | 1.45 | 0.671 | 1.477 | 0.119 | 1.358 | 0.003 | 111.1 | 6.7 |
| **14TS** | 2.041 | | 1.369 | | 1.385 | | 99.3 | |
| **14PR** | 2.781 | | 1.326 | | 1.373 | | 95.6 | |
| **14c** | 1.435 | 0.606 | 1.481 | 0.112 | 1.428 | 0.043 | 109.9 | 10.6 |

[a] Distances in Å; angles in degrees. All parameters computed by the G4 method except for those of the #PR structures which were optimized at the um062x level.

Interestingly, the structures of the "precursor" conformations were all quite chair like and resembled the TSs except that the $d_{1,5}$ distances were longer, the $d_{1,2}$ lengths were shorter (essentially unchanged double bonds) and the access angles varied. The distances from the radical centre X to C-5 of the alkene ($d_{1,5}$) in the TSs are in the range from 2.01 to 2.28 Å. The differences ($\delta d_{1,5}$) between $d_{1,5}$ in the TS and the analogous distances in the cyclized 5-member ring radicals are shown in column 3. The $d_{1,5}$ distances are somewhat longer for the *C*-centred radicals than for the *N*-centred and *O*-centred. Thus the slower cyclization rates of the *N*-centred radicals are not directly related to this aspect of orbital overlap. Similarly, there is no simple relationship between reactivity and the $d_{5,6}$ or $d_{1,2}$ structural parameters. The "access" angles $\theta_T$ vary from 104 to 111° in the TSs. The differences ($\delta\theta_T$) between $\theta_T$ in the TSs and the analogous angle in the cyclized radicals are listed in column 9 of Table 4. Intriguingly, a good linear correlation between $\delta\theta_T$ and the experimental activation parameters $E^{\ddagger}$ was observed (Figure 3). There was one notable outlying point for the **11e** system. A similar correlation was obtained with $\delta\theta_T$ values derived from the um062x computations. G4 computed $\delta\theta_T$ values also gave a reasonably linear correlation with the computed activation enthalpies ($\Delta H^{\ddagger}$) (see green circles in Figure 3) so the relationship has theoretical support. Excluding the outlier, the following relationship was obtained ($R^2$ = 0.958):

$$E^{\ddagger}\ (\text{kJ mol}^{-1}) = -3.50\times\delta\theta_T + 47.70 \qquad (3)$$

**Figure 3.** Plots of G4 computed $\delta\theta_T$ vs. activation parameters

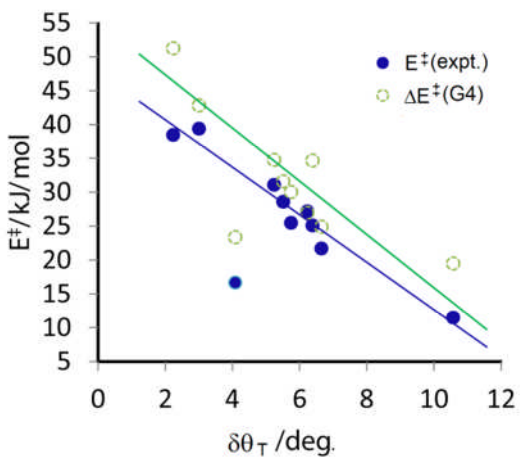


Equation (3) shows that large $\delta\theta_T$ correspond to fast cyclizations and small $\delta\theta_T$ to slow cyclizations with high activation energies. Naive analysis would expect the opposite, because small $\delta\theta_T$ might indicate the direction of approach of $X^{\bullet}$ in the TS would be favorable for overlap of the orbital on X with the alkene π-system. Evidently $\delta\theta_T$ represents some factor other than orbital overlap. A possibility was that small $\delta\theta_T$ could be indicative of chain stiffness and inflexibility with consequent slow molecular re-organization.

The 1-methylhex-5-enyl cyclizations **8e** (≡ **9e**) → **8c**(*trans*) + **9c**(*cis*) are particularly interesting. The data in Table 3 demonstrate that both the G4 and um062x methods *correctly yielded smaller* $\Delta H^{\ddagger}$ values for formation of **9c**(*cis*) even though this is more sterically crowded than **8c**(*trans*). The $\Delta H^{\ddagger}$ values of the G4 method in particular were within the error limits of the experimental data (compare with Table 1). The computed SOMO for **9TS** in Figure 2 strikingly illustrates that an extra attractive interaction between the alkene π-system and two of the methyl H-atoms is in operation in the TS of the *cis*-system. Thus the G4 (and um062x) computations gave some support for the idea of interaction between the hyperconjugatively delocalized SOMO and the alkene π* orbital as depicted in structure **4** and originally proposed by Beckwith and co-workers.[17]

This result naturally shifts attention to the *N*-methyl-pent-5-enylaminyl radical **5e** which contains a similar *cis/trans* structural feature to **8e** (≡ **9e**). The product 1-methylpyrrolidin-2-yl-methyl radical **5c** has, in principle, *trans*- and *cis*-isomeric forms. However, the pyramidyl *N*-atom undergoes rapid inversion at room temperature such that two isomers cannot be experimentally distinguished. The TS for cyclization of **5e** could adopt a *cis*- or *trans*-conformation. By analogy with **8e**, an extra attractive interaction between two of the *N*-Me H-atoms and the alkene π-system was anticipated for the *cis*-conformation. The computed activation enthalpies for cyclization of **5e** in Table 3 confirm this; the *trans*-TS was found to be 14 and 16 kJ mol$^{-1}$ higher in energy than the *cis*-TS by the G4 and um062x methods respectively. Furthermore, the SOMO of the **5TS(***cis***)** (compare with **9TS** in Figure 2) also illustrates the extension of the SOMO from the alkene π-system to the *N*-Me H-atoms rather well. The product radical **5c** will be undergoing rapid inversion of the N-atom, however, steric interaction between the 1,2-substituents will probably favor the *transoid* structure. In deriving the thermodynamic parameters for comparison with experiment it was assumed that the cyclization goes via the *cis*-TS to the *transoid* product radical.

Plots of the total energies computed at the um062x level vs the X·····C=C distance ($d_{1,5}$), are shown in Figure 4 for a selection *C*-, *N*- and *O*-centred radicals. These plots indicate that the activation barriers for the *N*-centred **5e** and **6e** are broader as well as higher than for the *C*-centred **7e**; as is that for the *O*-centred **13e**. For each cyclization a minimum was found in the region 2.8 to 3.4 Å corresponding to the "precursor" conformations of the open chain radicals. Figure 4 shows that for aminyl radical **5e** this precursor is situated further from the TS (larger $d_{1,5}$) and is higher in energy than for the archetypes **7e** and **14e**. This is an indication that the conformational re-organization of the chain of **5e**, so as to attain the chair Beckwith-Houk TS, may require more energy than for archetype **7e** or **14e**.

**Figure 4.** Plot of relative E(UHF) computed with the um062x functional vs. $d_{1,5}$

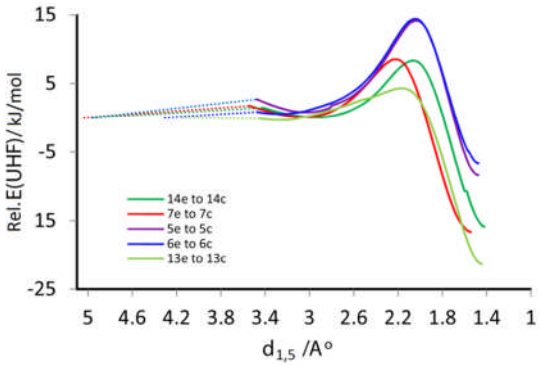


Red; hex-5-enyl system **7e**. Blue; aminyl system **5e**. Purple; iminyl system **6e**. Dark green; pentenyloxyl **14e**. Light green; allyloxycarbonyloxyl system **13e**.

Figure 5a and b show plots of the evolution along the reaction coordinate of the C=C bond lengths ($d_{5,6}$) and the ∠X····C=C = θ "access" angles of a selection of *5-exo* cyclizations. Examination of Figure 5(a) reveals that the alkene bond $d_{5,6}$ changes little for a good portion of the cyclization process for all the radicals.

For the *C*-centred radicals **7e** and **11e** interaction sets in at about 2.55 Å separation, for the *N*-centred radicals **5e** at about 2.35 Å and for the *O*-centred **14e** at about 2.33 Å. Since C-C bonds are intrinsically longer than C-N bonds which are longer than C-O bonds, the conclusion is that all three types behave in a similar, uniform manner. This, and their similar curvatures, implies that once the radical centre X• begins its interaction with the alkene, in effect is "captured" by the C=C double bond, all the radicals behave in an equivalent way in terms of overlap of the orbital on X with the π-system. It follows that this orbital overlap, or any other types of interaction of X• with the alkene, are not responsible for the higher and broader barriers of the N-centred species.

Figure 5(b), which charts the evolution of the "access" angle (θ), is very revealing in that most of the change is at longer $d_{1,5}$ distances where Figure 5(a) showed tranquility! For the *N*-centred radical **5e** the change in θ is "out of phase" with the alkene bond changes. The same is true of *N*-centred radical **6e** except that the trend is in the opposite direction. This is possibly related to imine-like character of the latter. The nearly horizontal red line for the *C*-centred **7e** (and **11e**) shows they maintain θ close to 109° even at distances where interaction with the π-system is negligible. Thus **7e** and **11e** are able to attain the conformation for optimum overlap with comparative ease.

**Figures 5(a) and (b).** Graph (a) shows the evolution of the C=C bond length ($d_{5,6}$) as a function of the reaction coordinate ($d_{1,5}$). Graph (b) shows the evolution of the access X····C=C angle (θ) as $d_{1,5}$ varies.

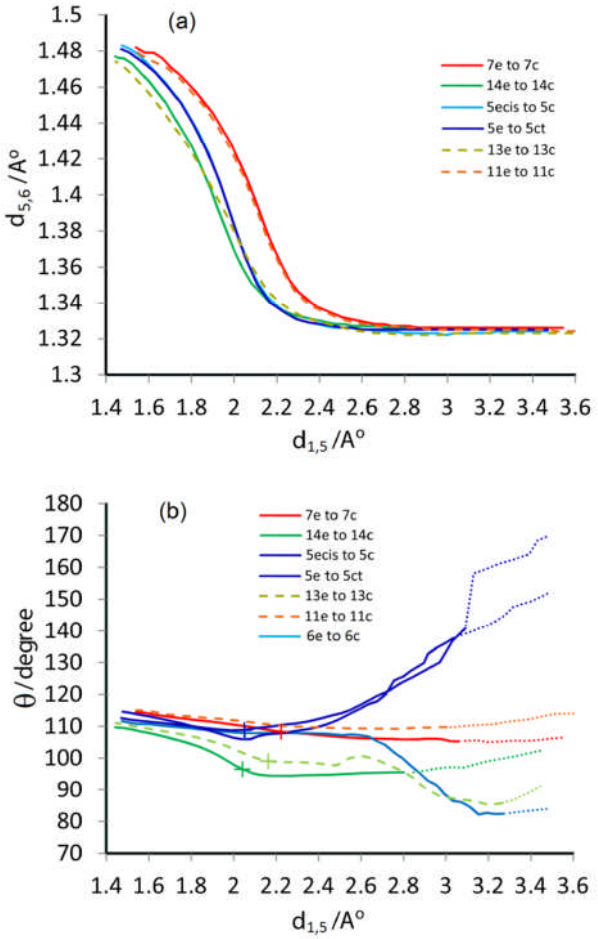


The crosses on Figure 5(b) mark the positions of the TSs. The transitions from full (or dashed) lines to dotted lines at longer $d_{1,5}$ mark the positions of the "precursor" conformations of the ring open radicals.

The blue lines for **5e(*cis*)** and **5e(*trans*)** indicate extensive conformational reorganization is required for these *N*-centred species. The *N*-centre approaches along a comparatively flat trajectory suggesting inflexibility of the chain at the C-N end and that energy needs to be expended during this stage of the reaction coordinate. This would certainly contribute to the higher and wider activation barrier found for the *N*-centred radical cyclizations. The light blue line for the iminyl radical trajectory (**6e**) indicates it approaches at large $d_{1,5}$ at comparatively acute angle; though again energy needs to be expended to attain the chair TS conformation. Its C=N bond is responsible for the inflexibility at the N-end of the chain and the acute angle is needed because iminyls are σ-radicals with their orbitals *in the plane* of the C=N π-system. An acute approach corresponds to roughly parallel π-systems of the C=N and C=C bonds which is conducive to overlap of the radical orbital which projects perpendicular to the C=N π-system.

The conformational inflexibility at the *N*-radical end of **5e** can probably be attributed to the availability of the extra pair of electrons on N as compared to $CH_2^{\bullet}$. These electrons are to be found in the penultimate occupied molecular orbital (POMO) which is shown for **5TS**, and compared with the *C*-centred **7TS** POMO in Figure 6.

**Figure 6.** Penultimate Occupied MOs for **5TS** and **7TS** Computed at the G4 level

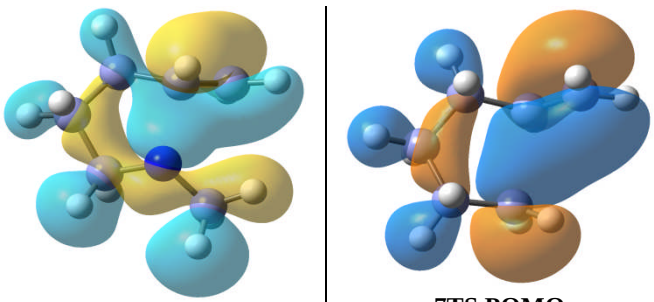

**5TS(*cis*) POMO** **7TS POMO**

Even though **5TS** occurs at short $d_{1,5}$, after the majority of the chain conformational reorganization, the POMO still shows a bonding lobe between N and C such that flexibility at this end of the chain will be restricted. A similar bonding lobe is present in the POMO of the GS open chain radical **5e**. The POMO for **7TS** on the other hand shows a node between the C-radical centre and the adjacent C-atom indicating free unrestricted conformational motion. It is worth mentioning that although the *O*-centred radical **14e** has four extra electrons the POMO for **14TS** doesn't show a bonding lobe between O and the adjacent C-atom (see ESI) so its conformational motion is not restricted in this way. The evolution of θ for *O*-centred radical **14e** (green line in Figure 5b) is comparatively level at longer $d_{1,5}$ consistent with little expenditure of energy on conformational reorganization.

The access angles $\theta_T$ of the TSs evidently reflect the conformational inflexibility/mobility at the radical end of the chains and this is manifested in the linear correlation obtained for $\delta\theta_T$ versus activation energy (Figure 3). The cyclization of the allyloxyethyl radical **11e** provides a very interesting test case. The O-substituent in this radical undoubtedly affects chain conformational mobility, but it is in the middle of the chain, away from the radical centre. The structure of the *C*-radical end of **11e** is virtually the same as for the archetype **7e** and, as Figure 5b shows (compare the red and orange lines), the evolution of θ with $d_{1,5}$ is very similar for the two species. For **11e** θ is too remote from the O-substituent to reflect its undoubted influence on the chain conformational reorganization. Thus $\delta\theta_T$ for **11e** does not measure this and the anomaly of the outlying point for **11e** in the correlations of Figure 3 is easily understood.

## Conclusions

G4 theory, and DFT theory with the um062x functional, gave good accounts of the *5-exo* cyclizations of radicals centred on first row elements. That *N*-centred radicals ring close more slowly than *C*-centred and *O*-centred was correctly predicted. Both methods also predict, in agreement with experiment, that 1-methyl-hex-5-enyl radicals (**8e**, **9e**) and *N*-methyl-pent-5-enylaminyls (**5e**) will preferentially ring close to give *cis*-1,2-disubstituted rings. The "access" angles ∠X·····C=C = θ were discovered to be critical parameters. Plots of the evolution of θ with the double bond extension ($d_{5,6}$) along the reaction coordinate, showed the two were "out of phase" for *N*-centred radicals. This, and other evidence, supported the conclusion that the comparatively slow ring closure of the *N*-centred radicals was due to lack of flexibility at the N-ends of their chains. This meant that extra energy was expended in attaining their chair-like TSs with consequent increases in the width and height of the activation barriers. Interestingly, the access angle in the TS ($\theta_T$) reflected this factor such that linear correlations of $\delta\theta_T$ with both experimental Arrhenius activation energies and computed activation enthalpies were observed. These only held true, however, of radicals with all-methylene chains.

## Acknowledgements

I thank the EPSRC (grant EP/I003479/1) and EaStCHEM for funding. I am grateful to Dr. Herbert Fruchtl and Prof. Michael Bühl for help with the computing.

## Notes and references

[a] University of St. Andrews, EaStCHEM School of Chemistry, St. Andrews, Fife, UK, KY16 9ST. E-mail: jcw@st-and.ac.uk; Tel. 44 (0)1334 463864; Fax 44 (0)1334 463808.

† Electronic Supplementary Information (ESI) available: graphics of SOMOs of principal species, Cartesian coordinates of optimised GS and TS structures. See DOI: 10.1039/b000000x/

1. For reviews see: (a) P. Renaud and M. P. Sibi, eds. *Radicals in Organic Synthesis*; Wiley-VCH: Weinheim, 2001; (b) C. Chatgilialoglu and A. Studer, eds. *Encyclopedia of Radicals in Chemistry Biology and Materials*; Volume 2, *Synthetic Strategies and Applications;* Wiley, 2012, DOI: 10.1002/9781119953678 available online: http://onlinelibrary.wiley.com/book/10.1002/9781119953678 (accessed 21/05/2014); (c) A. G. Fallis and I. M. Brinza, *Tetrahedron*, 1997, **53**, 17543
2. (a) C. P. Jasperse, D. P. Curran and T. L. Fevig, *Chem. Rev.* 1991, **91**, 1237; (b) W. R. Bowman, C. F. Edge and P. Brookes, *Chem. Soc. Rev.* 2000, 1; (c) D. J. Hart, In *Radicals in Organic Synthesis*; P. Renaud and M. P. Sibi, Eds.; Wiley-VCH: Weinheim, 2001; Volume 2, pp 279-302; (d) E. Lee, In *Radicals in Organic Synthesis*; P. Renaud and M. P. Sibi, Eds.; Wiley-VCH: Weinheim, 2001; Volume 2, pp. 303; (e) T. Taniguchi and H. Ishibashi, *Heterocycles*, 2013, **87**, 527.
3. (a) R. A. Bunce, *Tetrahedron*, 1995, **51**, 13102; (b) A. J. McCarroll and J. C. Walton, *Angew. Chem. Int. Ed.* 2001, **40**, 2224; (c) M.

Albert, L. Fensterbank, E. Lacote and M. Malacria, *Top. Curr. Chem.* 2006, **264**, 1; (d) A. Baralle, A. Baroudi, M. Daniel, L. Fensterbank, J.-P. Goddard, E. Lacote, M.-H. Larraufie, G. Maestri, M. Malacria and C. Ollivier, In *Encyclopedia of Radicals in Chemistry, Biology and Materials*, Volume 2, *Synthetic Strategies and Applications;* C. Chatgilialoglu and A. Studer, Eds.; Wiley, 2012, **2**, 729-765; available online: http://onlinelibrary.wiley.com/book/10.1002/9781119953678 (accessed 21/05/2014).

4. A. L. J. Beckwith and K. U. Ingold, In *Rearrangements in Ground and Excited States*, F. de Mayo, Ed.; Academic Press: New York, 1980, Vol. 1, 161.
5. M. Newcomb, *Tetrahedron*, 1993, **49**, 1151.
6. M. Newcomb, In *Encyclopedia of Radicals in Chemistry, Biology and Materials*, Volume 2, *Synthetic Strategies and Applications;* C. Chatgilialoglu and A. Studer, Eds.; Wiley, 2012, available online: http://onlinelibrary.wiley.com/book/10.1002/9781119953678 (accessed 21/05/2014).
7. C. E. Brown, A. G. Neville, D. M. Rayner, K. U. Ingold and J. Lusztyk, *Aust. J. Chem.* 1995, **48**, 363.
8. C. Chatigilialoglu, C. Ferreri, M. Lucarini, A. Venturini and A. A. Zavitsas, *Chem. Eur. J.* 1997, **3**, 376.
9. O. M. Musa, J. H. Horner, H. Shahin and M. Newcomb, *J. Am. Chem. Soc.* 1996, **118**, 3862.
10 M. Newcomb, O. M. Musa, F. M. Martinez and J. H. Horner, *J. Am. Chem. Soc.* 1997, **119**, 4569.
11. R. T. McBurney and J. C. Walton, *J. Am. Chem. Soc.* 2013, **135**, 7349.
12. M.-H. Le Tadic-Biadatti, A.-C. Callier-Dublanchet, J. H. Horner, B. Quiclet-Sire, S. Z. Zard and M. Newcomb, *J. Org. Chem.* 1997, **62,** 559.
13. F. Portela-Cubillo, R. Alonso-Ruiz, D. Sampedro and J. C. Walton, *J. Phys. Chem. A* 2009, **113**, 10005.
14. J. Hartung and F. Gallou, *J. Org. Chem.* 1995, **60**, 6706.
15. J. Hartung, K. Daniel, C. Rummey and G. Bringmann, *Org. Biomol. Chem*. 2006, **4**, 4089.
16. R. T. McBurney, A. D. Harper, A. M. Z. Slawin and J. C. Walton, *Chem. Sci.* 2012, **3**, 3436.
17. A. L. J. Beckwith, I. Blair and G. Phillipou, *J. Am. Chem. Soc.* 1974, **96**, 1613.
18. A. L. J. Beckwith and C. H. Schiesser, *Tetrahedron* 1985, **41**, 3925.
19. D. C. Spellmeyer and K. N. Houk, *J. Org. Chem*. 1987, **52**, 959.
20. A. H. C. Horn and T. Clark, *J. Am. Chem. Soc*. 2003, **125**, 2809.
21. P. d'Antuno, A. Fritsch, L. Ducasse, F. Castet, P. James and Y. Landais, *J. Phys. Chem. A*, 2006, **110**, 3714.
22. C. M. Jäger, M. Hennemann, A. Mieszała and T. Clark, *J. Org. Chem*. 2008, **73**, 1536.
23. A. R. Matlin and M. C. Leyden, *Int. J. Org. Chem.* 2013, **3**, 169.
24. J. A. R. Luft, T. Winkler, F. M. Kessabi and K. N. Houk, *J. Org. Chem*. 2008, **73**, 8175.
25. A. N. Hancock and C. H. Schiesser, *Chem. Sci.* 2014, **5**, 1967.
26. F. Liu, K. Liu, X. Yuan and C. Li, *J. Org. Chem*. 2007, **72**, 10231.
27. J. C. Walton, *Acc. Chem. Res.* 2014, **47**, 1406.
28. C. Chatgilialoglu, K. U. Ingold and J. C Scaiano, *J. Am. Chem. Soc.* 1981, **103**, 7739.
29. J. Lusztyk, B. Maillard, S. Deycard, D. A. Lindsay and K. U. Ingold, *J. Org. Chem.* 1987, **52**, 3509.
30. A. L. J. Beckwith and S. Glover, *Aust. J. Chem.* 1987, **40**, 157.
31. C. Chatgilialoglu, D. Crich, M. Komatsu and I. Ryu, *Chem. Rev.* 1999, **99**, 1991.
32. M. J. Frisch, et al. Gaussian 09, Revision C 1, Gaussian, Inc., Wallingford CT, 2009 (See ESI for full citation).
33. T. H. Dunning, Jr. *J. Chem. Phys.* 1989**, 90** 1007.
34. R. A Kendall, T. H. Dunning, Jr. and R. J. Harrison, *J. Chem. Phys.* 1992, **96**, 6796.
35. J. A. Montgomery, Jr. M. J. Frisch, J. W. Ochterski and G. A. Petersson, *J. Chem. Phys.* 2000, **112**, 6532.
36. Y. Zhao, N. González-Garcia and D. G. Truhlar, *J. Phys. Chem. A*, 2005, **109**, 2012.
37. L. A. Curtiss, P. C. Redfern and K. Raghavachari, *J. Chem. Phys.* 2007, **126,** 084108-1-084108-12.
38. Y. Zhao and D. G. Truhlar, *Theor. Chem. Acc.* 2008, **120**, 215.
39. A. A. Zavitsas, In *Encyclopedia of Radicals in Chemistry, Biology and Materials*, Volume 2, *Synthetic Strategies and Applications;* C. Chatgilialoglu and A. Studer, Eds.; Wiley, 2012, *1,* available online: http://onlinelibrary.wiley.com/book/10.1002/9781119953678 (accessed 21/05/2014).
40. A. A. Zavitsas, N. Matsunaga and D. W. Rogers, *J. Phys. Chem. A*, 2008, **112**, 5734.
41. I. A. Alubagin and M. Manoharan, *J. Am. Chem. Soc.* 2005, **127**, 12583.
42. I. A. Alabugin, K. Gilmore and M. Manoharan, *J. Am. Chem. Soc.* 2011, **133**, 12608.

 